Resource

Application of Active and Kinase-Deficient Kinome Collection for Identification of Kinases Regulating Hedgehog Signaling

Markku Varjosalo,[1,2,3,8] Mikael Björklund,[1,2,3,8] Fang Cheng,[2] Heidi Syvänen,[1,2,3] Teemu Kivioja,[1,2,4] Sami Kilpinen,[2,5] Zairen Sun,[6] Olli Kallioniemi,[2,5] Hendrik G. Stunnenberg,[7] Wei-Wu He,[6] Päivi Ojala,[2,*] and Jussi Taipale[1,2,3,*]

[1]Department of Molecular Medicine, National Public Health Institute (KTL), FI00290 Helsinki, Finland
[2]Genome-Scale Biology Program, Biomedicum Helsinki, Institute of Biomedicine
[3]High Throughput Center
[4]Department of Computer Science
University of Helsinki, PO Box 63, FI-00014, Finland
[5]Medical Biotechnology Center, VTT Technical Research Centre of Finland and University of Turku, Itäinen Pitkäkatu 4A, FI-20520 Turku, Finland
[6]OriGene Technologies Inc, Six Taft Court, Suite 100, Rockville, MD 20850, USA
[7]Department of Molecular Biology, Radboud University Nijmegen, P.O. Box 9101, 6500 HB Nijmegen, The Netherlands
[8]These authors contributed equally to this work.
*Correspondence: paivi.ojala@helsinki.fi (P.O.), jussi.taipale@helsinki.fi (J.T.)
DOI 10.1016/j.cell.2008.02.047

SUMMARY

To allow genome-scale identification of genes that regulate cellular signaling, we cloned >90% of all human full-length protein kinase cDNAs and constructed the corresponding kinase activity-deficient mutants. To establish the utility of this resource, we tested the effect of expression of the kinases on three different cellular signaling models. In all screens, many kinases had a modest but significant effect, apparently due to crosstalk between signaling pathways. However, the strongest effects were found with known regulators and novel components, such as MAP3K10 and DYRK2, which we identified in a mammalian Hedgehog (Hh) signaling screen. DYRK2 directly phosphorylated and induced the proteasome-dependent degradation of the key Hh pathway-regulated transcription factor, GLI2. MAP3K10, in turn, affected GLI2 indirectly by modulating the activity of DYRK2 and the known Hh pathway component, GSK3β. Our results establish kinome expression screening as a highly effective way to identify physiological signaling pathway components and genes involved in pathological signaling crosstalk.

INTRODUCTION

Protein kinases are one of the largest families of genes in eukaryotes: approximately 2% of all human genes have protein kinase domain(s) (Venter et al., 2001). Protein kinases mediate most of the signal transduction events in cells by phosphorylation of specific substrates—modifying their activity, cellular location, and/or association with other proteins. Mammalian protein kinases can be divided into tyrosine kinases, serine/threonine kinases, and kinases that can phosphorylate both tyrosine and serine/threonine residues. Despite these differences in substrate specificity, all known mammalian protein kinases have structurally similar kinase domains (Huse and Kuriyan, 2002; Nolen et al., 2004).

The kinase domain is composed of 250–300 amino acid residues and can be divided into two subdomains, a smaller N lobe and a larger C lobe, between which is the cleft into which ATP and substrates bind (Huse and Kuriyan, 2002; Nolen et al., 2004). The relatively strong conservation of kinase domains has allowed the computational characterization of the protein kinase complement of the human genome (the kinome), and for most kinases, also the identification of critical residues required for their catalytic activity (Manning et al., 2002). These residues include a lysine (Lys72 in PKA) in the N lobe, which is required for proper orientation of ATP, and an aspartate (Asp166 in PKA) in the catalytic loop, which interacts with the hydroxyl side chain of the substrate (Huse and Kuriyan, 2002). Mutations in these residues kill the catalytic activity of kinases (Manning et al., 2002), but do not interfere with substrate recognition or binding to other proteins. As a result, catalytically inactive kinase can either have no activity, or dominant-negative activity due to titration of cofactors from the corresponding active kinase (Mendenhall et al., 1988).

Protein kinases are the most common class of genes among known cancer genes. In most cases, cancer is associated with increase in activity of specific kinases caused by mutational activation, or increase in expression due to gene amplification or translocation (Futreal et al., 2004). In a recent study, ∼23% (120/518) of kinase genes were estimated to function as cancer genes (Greenman et al., 2007). An unexpectedly large number of kinases were found to be mutated, but in many cases at a relatively low frequency, suggesting that either a large number of kinase

pathways can contribute to cancer or that many kinases can regulate the same pathways when activated unphysiologically.

To allow unbiased genome-wide analysis of crosstalk between kinase pathways and the role of kinases in cellular signaling, we developed a collection of >93% of full-length human protein kinase cDNAs. Because increased kinase expression often leads to gain-of-function phenotypes due to increased activity, this collection could be used to systematically screen for kinases affecting a given cellular phenotype. However, because overexpression can also lead to loss-of-function effects due to scaffolding or other nonenzymatic functions of kinases, we also generated a corresponding set of catalytically inactive kinases, which can be used to test whether the kinase activity is required for the observed phenotypes. To test the utility of this resource, we performed a set of screens designed to identify novel kinases affecting oncogenic signaling pathways.

Of particular interest to us was the Hh signaling pathway (Varjosalo and Taipale, 2007), because it has been linked to several forms of human cancer (Rubin and de Sauvage, 2006). In addition, we and others have recently found that some components, including the protein kinase Fused, that regulate this signaling pathway in invertebrate model organisms do not affect Hh signaling in mammals (Chen et al., 2005; Cooper et al., 2005; Merchant et al., 2005; Svard et al., 2006; Varjosalo et al., 2006), suggesting that kinases distinct from Fused regulate Shh (Sonic hedgehog, a mammalian ortholog of Hh) pathway activity. To identify such kinases, we screened the kinase collection in a cell-culture model of Shh signaling, finding two novel kinases regulating the Shh pathway, DYRK2 and MAP3K10. Both of these kinases were also required for Shh signaling, as revealed by a kinome-wide siRNA screen. Using cell lines deficient in different components of the Shh pathway, we further mapped the activities of these kinases to the GLI transcription factors, and showed that they are required for pathway function in cultured cells and also affected Shh signaling in vivo.

To further validate the kinome resource, and to test the specificity of the kinases identified as Shh effectors, we also performed two other screens: a TGFβ signaling screen and a screen for activators of replication of latent Kaposi's sarcoma herpes virus (KSHV). Whereas the TGFβ screen identified only known effectors, the KSHV screen linked a novel kinase, PIM1, to activation of virus replication. Upon treatment of cells with viral activators, PIM1 expression was induced, and the kinase associated with and phosphorylated the KSHV latency-associated nuclear antigen 1 (LANA-1), resulting in activation of lytic gene expression.

These results show that the genome-wide collection of protein-kinase cDNAs we describe here can be used to systematically and quantitatively analyze signaling crosstalk, and also to identify novel regulatory kinases in multiple cellular signaling models.

RESULTS

Generation of Kinome-wide Expression-Ready cDNA Library

The initial set of full-length kinase cDNAs were isolated from ~800,000 individual sequenced cDNA clones derived from 20 different tissues. Subsequently, cDNAs for the kinases that were not identified by brute force sequencing were isolated by PCR screening of pooled and plated libraries (Figure 1A; Table S1). The resulting 568 genome-wide full-length kinome cDNA array constructs are based on the pCMV6-XL vector (GenBank: AF067196) that contain a CMV promoter, and a SV-40 origin of replication for episomal replication and very strong overexpression in cells expressing the SV-40 large T antigen (e.g., 10^5–10^6 proteins/cell in COS1 cells) (Taipale et al., 2002). In cells lacking SV-40T, the vector does not replicate, but the efficient CMV promoter leads to the expression of proteins at moderate to high levels (e.g., 10^3–10^4 proteins/cell) (Taipale et al., 2002), resulting in overexpression of most nonstructural proteins.

We next used direct PCR to attempt to clone all of the remaining kinases from five separate sources of cDNA, representing 48 different tissues and 34 unique cell lines. Using this approach, 16 more kinases were cloned, bringing the total to 93% of all human kinases identified in silico (Manning et al., 2002). Analysis of the remaining 36 kinase ORFs, which we could not clone, revealed that many of these were of very large size (13 are >1500 aa, including titin and obscurin), or were expressed at very low or neglible levels or in a very narrow range of tissues (15 kinases; Table S1). Failure to clone the remaining kinases could also be due to toxicity in *E.coli*, or problems with gene annotation. Three kinases are not included in current ENSEMBL gene annotation, and there is no experimental evidence to support the in silico predicted human full-length ORFs for 26 of the 36 remaining kinases (Table S1).

Taken together, the resulting human kinome collection consists of 568 cDNAs, representing 480 different kinases. The representation of the different kinase subfamilies defined by Manning et al. (2002) are shown in Figure 1B.

Analysis of Splice Forms and Protein Expression

Many kinases have alternatively spliced forms, some of which code for functionally distinct, truncated and/or inactive proteins. To address whether the splice forms present in our collection are representative of the active kinome, we identified known protein domains contained in the splice forms found in our collection, and compared these to domains found in all splice forms of the same kinases. Based on ENSEMBL annotations, we could identify 1484 potential splice forms for our kinase clones, containing a total of 1725 protein domains. The clones of our collection contained the vast majority (1692; 98.1%) of these domains (see Supplemental Database).

The initial clone collection contains native untagged kinases, ensuring wild-type activity, but making protein analyses dependent on antibodies, which exist only against a minority of kinases. To validate that the constructs express protein, we performed an unbiased sampling using all immunohistochemistry-grade kinase antibodies available from one supplier. Of 18 tested constructs, 12 expressed protein (Figure 1C), and expression of the remaining 6 could not be verified due to nonreactivity of the antibody (nonreactivity against V5-tagged kinases; not shown).

To analyze a larger sample, we transferred 328 kinase ORFs lacking stop codons to a Gateway recombination cloning entry vector and moved 212 of these to a recipient vector containing a C-terminal triple-V5 epitope tag (Table S1), and tested the expression of this unbiased subset in COS1 cells. Transfection of eight of these constructs was toxic to COS1 cells. Dot-immunoblot analysis indicated that of the remaining 204
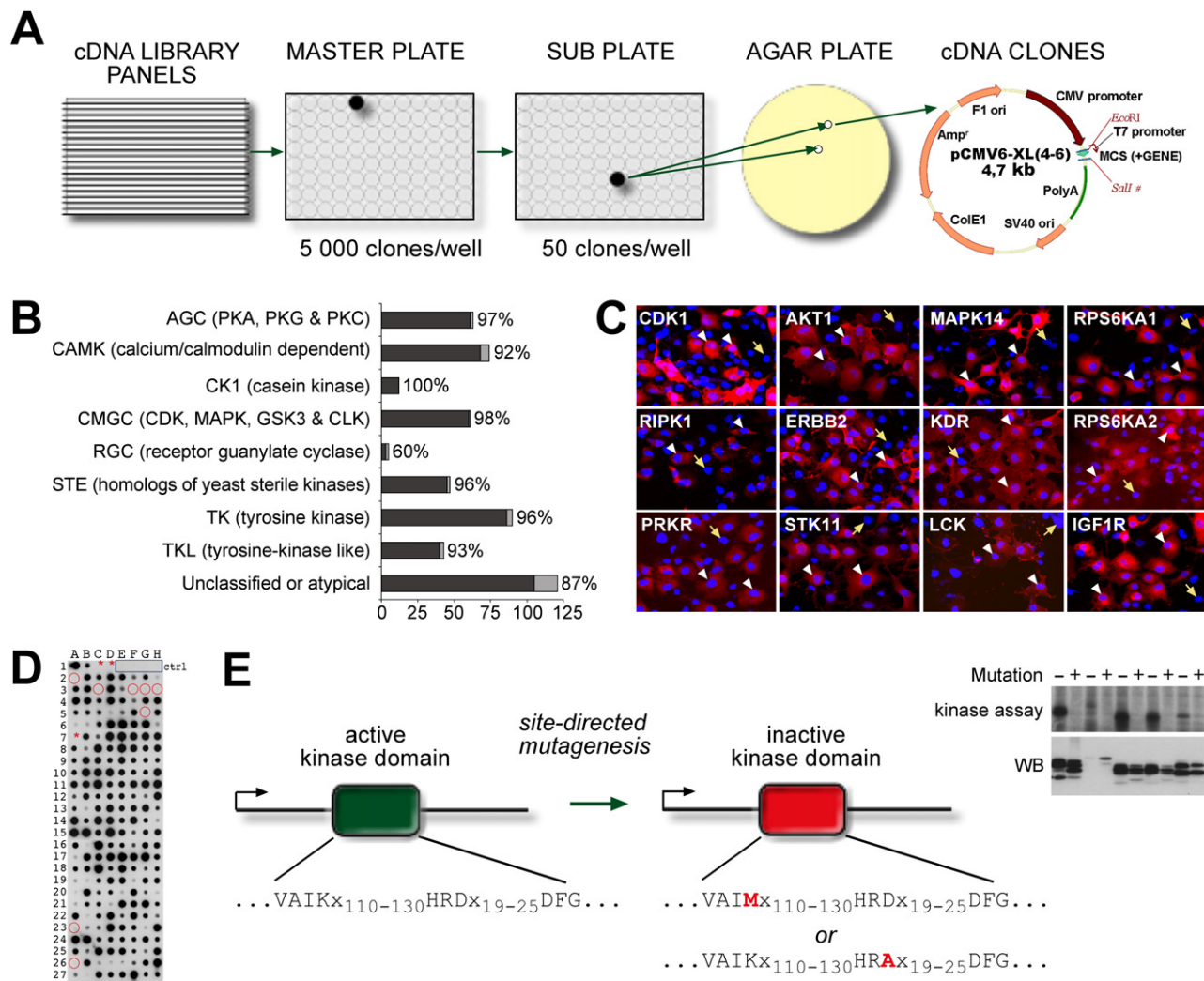
Figure 1. Kinase Cloning

(A) cDNAs were identified by screening master plates containing 5000 clones/well by PCR followed by subsequent PCR screening of lower-density subplates.

(B) Coverage of kinases in different subclasses (Manning et al., 2002).

(C) Validation of cDNA expression. cDNA expressing (white arrowheads) and nonexpressing (yellow arrows) COS1 cells were identified by specific antibodies against the indicated kinases (red staining; DNA is stained blue).

(D) Dot immunoblot of lysates of COS1 cells expressing 212 kinases with C-terminal triple-V5 tags. Mock-transfected controls (blue box), kinases with clear toxicity (red circles), and nonexpressing kinases (red asterisk) are indicated.

(E) Kinase cDNAs (left) were mutated using site-directed mutagenesis to generate kinase-deficient constructs (right). Mutated residues (red) in active-site motifs are indicated. Lower conservation is indicated by x. Inset shows kinase assays of COS1 cell-expressed active and inactivated kinases. For identities of kinases in (C)–(E), see Table S1.

constructs, 201 (98.5%) expressed protein at detectable level, and 3 (1.5%) failed to express (Figure 1D).

Taken together, these analyses indicate that the kinase collection cDNAs contain nearly all annotated protein domains found in the respective genes, and that the vast majority of the kinase constructs tested express full-length protein.

Generation of Catalytically Inactive Kinase cDNA Collection

Kinase expression can affect cellular phenotype due to increased catalytic activity or due to scaffolding or other functions of the kinase protein. To differentiate between these possibilities, kinases with active site mutations are commonly used; however, no large collection of such inactive kinases is available. To facilitate the downstream analysis of the kinases identified in various screens, we designed oligonucleotides for site-directed mutagenesis of critical residues of the kinase domains of all the kinases that were predicted to be catalytically active (Table S2) and performed high-throughput mutagenesis. The resulting catalytically inactive kinome library (Table S2) contains 425 kinase cDNAs, representing 351 unique inactive kinases. Of these, 390 (316 unique kinases) were generated by mutagenesis, and
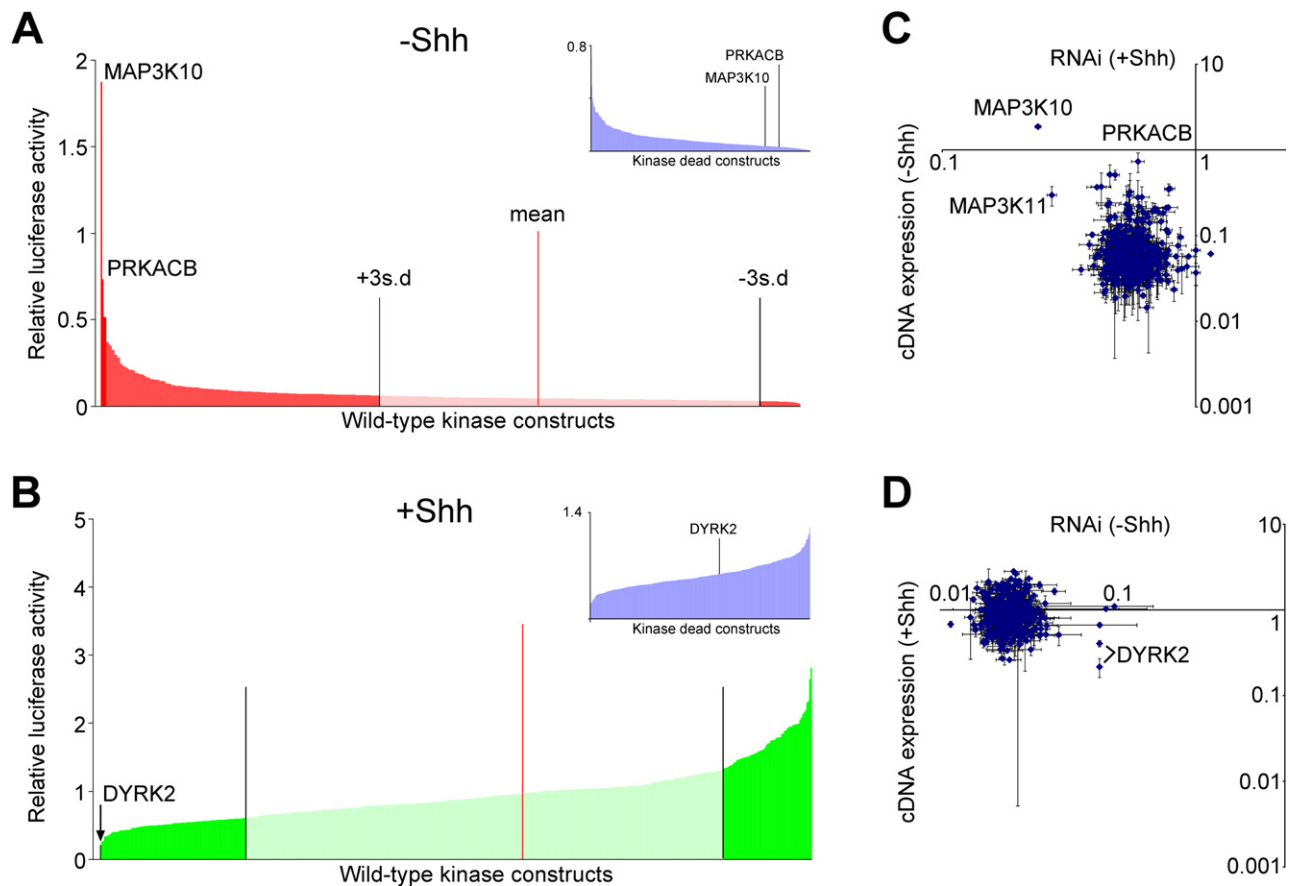
Figure 2. Kinase cDNA and RNAi Screen for Novel Shh Pathway Components

(A and B) Effect of kinase expression on Shh pathway activity in the absence (A) or presence (B) of ShhN. Samples are sorted by phenotypic score. Red bars indicate means, and black bars ±3 SD calculated from control samples (99.7% confidence, <1 false positive sample expected above and below 3 SD). Samples that significantly differ from the mean are indicated by darker color; names of the kinases with strongest activities are also shown. Insets (top right) show ranks of MAP3K10, PRKACB, and DYRK2 in corresponding screens performed using kinase-deficient constructs.

(C) MAP3K10 is required for Shh signaling. An x-y plot of results from kinome cDNA (y axis) and RNAi (x axis) screens that illustrates positive regulators of the Shh pathway.

(D) DYRK2 is required for Shh signaling. An x-y plot of kinome cDNA and RNAi screens that illustrates negative regulators of the Shh pathway. The two data points for DYRK2 are due to the presence of a single siRNA pool but two different cDNA constructs in the respective screens. Note that MAP3K10 and DYRK2 are strong effectors in both cDNA and RNAi screens. For numerical data, see Tables S3 and S4. Error bars indicate 1 SD (n = 3).

in the remaining 35 cases, the wild-type kinase lacks critical catalytic residues and is predicted to be inactive. In most of the mutant kinases (313 of 316), the lysine in the "VAIK" motif (Lys72 of PKA) (Manning et al., 2002) was mutated to methionine (Figure S1). If the lysine was absent or could not be unequivocally identified (three kinases), the aspartate in the "HRD" motif (Asp166 of PKA) was mutated to alanine.

To validate the activity of the kinase collection and to confirm effectiveness of the kinase-inactivating mutations, we analyzed an unbiased sample consisting of 84 pairs of wild-type and mutant kinases expressed in COS1 cells by in vitro kinase assays. Eighty-two percent of the wild-type kinase precipitates had detectable kinase activity (Table S2). This is likely an underestimate of the fraction of active kinases, as specific substrates for most kinases are not known. Specificity of kinases is illustrated by the fact that a smaller fraction (70%) of the kinases had autophosphorylation activity, and only 19% displayed activity toward

a commonly used substrate (casein). Ninety-five percent of kinases showing robust activity in wild-type form were inactivated by the lysine mutation (Table S2; Figure 1E).

A Large Fraction of All Kinases Significantly Affect Shh Signaling

To test the utility of the kinome resource for identifying novel genes relevant to cancer, we applied it to overexpression screening in multiple cell-based models. We first analyzed Shh signaling in NIH 3T3 cells (Taipale et al., 2000) by transfecting the cells in triplicate with each kinase expression construct together with the Shh-responsive reporter GLI-Luc (Taipale et al., 2002). Analysis of the data revealed that 320 kinase constructs significantly (± 3 standard deviation [SD]) affected either the uninduced or Shh-induced pathway activity (Figures 2A and 2B; Table S3). In addition to PKA (Kalderon, 2005), it has been previously suggested on the basis of overexpression

experiments that mammalian Hh signaling is specifically affected by four protein kinases: DYRK1, PKCδ, ERK-1, and AKT/PKB (Mao et al., 2002; Riobo et al., 2006a, 2006b). Of these, we did not observe an effect by overexpression of PKCδ, but found that ERK-1, AKT1, and DYRK1 class kinase (DYRK1B) had statistically significant effects on Shh signaling (Table S3). The effect of DYRK1B was relatively strong, whereas >90 kinases had equal or stronger activity than ERK-1 or AKT1.

Relatively Few Kinases Have Strong Effect on Shh Signaling

Although many kinases had small but significant effects on Shh-specific reporter, expression of only four kinases—MAP3K10, PKA, STK23, and PIM1—resulted in reporter activity that was more than 75% of that induced by Shh, and only one kinase, DYRK2, inhibited Shh-induced reporter activity more than 75%. Importantly, PKA, which depending on the dose either positively or negatively affects Hh signaling in *Drosophila* (Zhou et al., 2006), was among the strongest effectors. STK23 and PIM1, but not MAP3K10 or DYRK2, also activated a mutant GLI site-containing reporter (Figure S2A), indicating that their effects on the reporter activity were not mediated by the Shh pathway.

We next analyzed whether the kinase activities of MAP3K10 and DYRK2 were required for their activity by transfecting the catalytically inactive kinome collection to NIH 3T3 cells together with the GLI-Luc reporter. This analysis revealed that the kinase activities of both MAP3K10 and DYRK2 were critical for their ability to regulate the Shh pathway (insets in Figures 2A and 2B; Figure S2B).

To test whether the kinases were necessary for normal Shh pathway function, we screened a siRNA library targeting the mouse kinome in Shh-LIGHT2 cells (Taipale et al., 2000) in the presence and absence of Shh. siRNAs targeting Map3k10 decreased the level of Shh-induced pathway activity (Figure 2C), whereas siRNAs targeting Dyrk2 resulted in activation of the Shh pathway in the absence of ligand (Figure 2D), indicating that both kinases are required for Shh signaling. The siRNA data were further validated using shRNA constructs to rule out off-target effects (Figure S2C).

Analysis of Signaling Specificity

To test the specificity of the kinases, we performed a similar screen to identify cellular kinases that activate lytic replication of a latent tumor virus KSHV—the causative agent of Kaposi's sarcoma and primary effusion lymphoma (Cesarman et al., 1995; Chang et al., 1994). To perform the screen, the kinases were transfected to Vero cells infected with a recombinant KSHV expressing RFP from the lytic PAN promoter (Vieira and O'Hearn, 2004), and viral reactivation was primed by expression of the viral transactivator RTA from a baculoviral vector. Quantification of the RFP intensities revealed that only one kinase, PIM1, induced viral reactivation in two independent experiments (Figure 3A). Conversely, kinase-deficient PIM1 acted in a dominant-negative fashion, decreasing the basal level of reactivation (Figure 3A). In addition, a chemical stimulator of viral reactivation, sodium butyrate, induced expression of endogenous PIM1, and association of PIM-1 with LANA-1, a protein that is required for

maintenance of viral latency. PIM1 also phosphorylated LANA-1, resulting in activation of viral lytic gene expression (Figure 3B). These results suggest that PIM1 mediates viral reactivation via phosphorylation of LANA-1.

To further establish the specificity of the screening method, we performed another luciferase reporter-based screen to identify effectors of TGFβ signaling in mink lung Mv1Lu cells (Dennler et al., 1998). The kinases with the strongest effects in this screen were clearly distinct from those identified in the Shh and KSHV screens, and included type I and type II receptors (Massague et al., 2005) for activin and TGFβ (Figures 3C and 3D; Table S5). Taken together, the three kinome-wide screens clearly establish that although many kinases can cause crosstalk when overexpressed, the strongest effectors identified are specific. Thus, expression screening can be used to identify both known and novel kinases affecting cellular signaling processes.

Validation of Shh Pathway-Specific Effects of DYRK2 and MAP3K10

We next set out to further characterize the mechanism of action of the novel kinases affecting the Shh pathway, DYRK2 and MAP3K10. First, we determined their expression pattern by systematic analysis of existing microarray expression data. This analysis revealed that these kinases are expressed in most normal tissues analyzed; MAP3K10 expression is highest in the lymphatic system, heart and bone marrow, whereas DYRK2 expression is strong in lymphatic system and in muscle-rich tissues, such as skeletal muscle and heart (Figure 3E; Table S6). The subcellular localization of GFP-tagged biologically active DYRK2 and MAP3K10 was cytoplasmic, suggesting that they regulate a cytoplasmic component of the Shh pathway (Figure S3).

DYRK2 and MAP3K10 Have a Role in Shh Signaling In Vivo

To test whether DYRK2 and MAP3K10 also affect the Shh pathway in vivo, we expressed them in chick neural plate using in ovo electroporation, and analyzed their effect on Shh signaling using well-described markers (Jacob and Briscoe, 2003) for cells exposed to high (FoxA2+), medium (Nkx2.2+), or low (Pax7−) levels of Shh (Figures 4A–4I and S3). Expression of MAP3K10 induced high levels of Shh signaling, as indicated by its ability to induce ectopic dorsal expression of FoxA2 (Figures 4D–4F and S3). Expression of DYRK2, in contrast, suppressed Shh signaling, as indicated by its ability to block ventral expression of Nkx2.2 (Figure 4J). These results indicate that MAP3K10 and DYRK2 can affect the Shh pathway both in cultured NIH 3T3 fibroblasts and in developing neural cells in vivo.

DYRK2 and MAP3K10 Act at the Level of the GLI Transcription Factors

To genetically map where these kinases act on the Shh pathway, we used cells overexpressing or deficient in specific Shh pathway components. First, we tested the ability of these kinases to function in cells where the transducing component of the Shh receptor, Smo, was hyperactive or genetically ablated. DYRK2 could inhibit the Shh pathway in the presence of oncogenically activated Smo (SmoA1) (Taipale et al., 2000) (Figure S4A), suggesting that it acts at or downstream of Smo. Similarly, MAP3K10 was
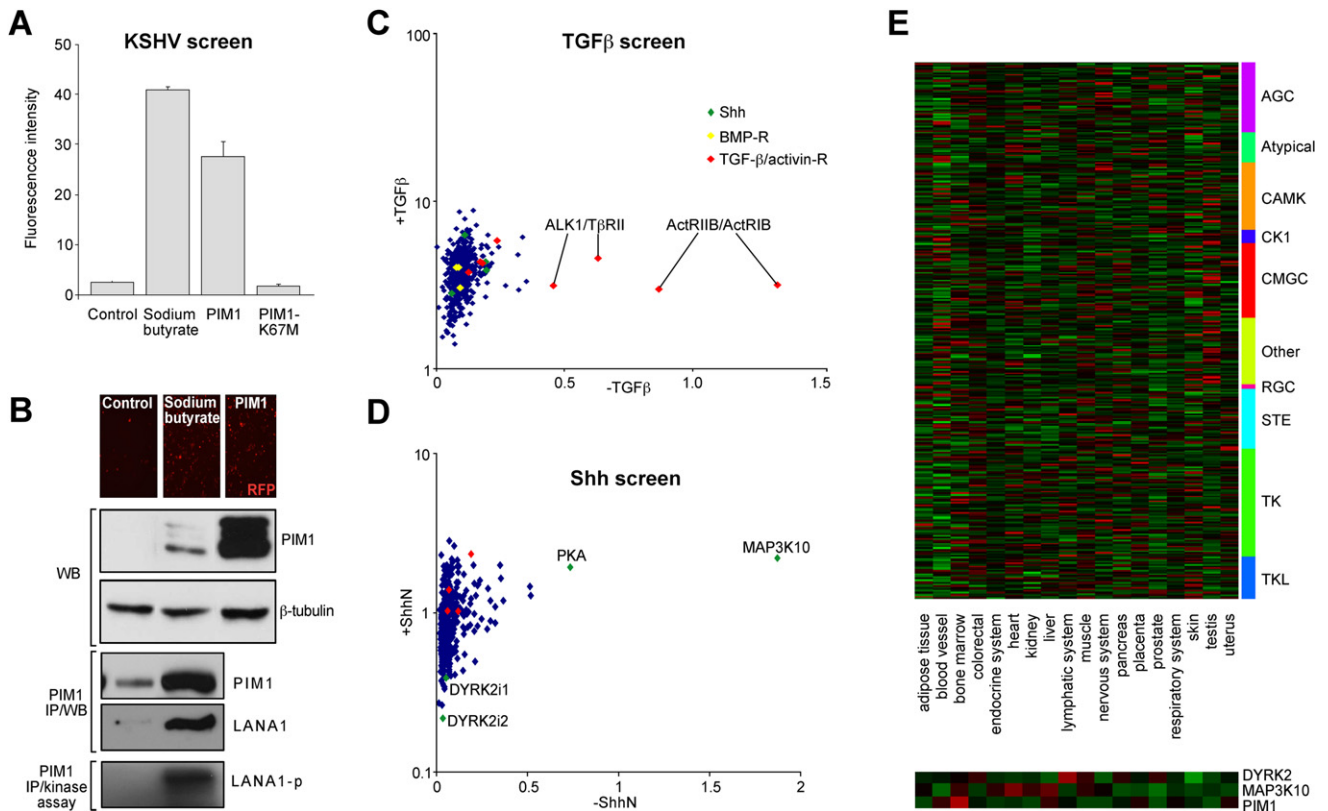
Figure 3. Specificity of Overexpression Screening

(A–D) Three different kinome screens identify distinct kinases as strongest effectors, indicating that the effects of the overexpression of MAP3K10 and DYRK2 are specific for the Shh pathway. In (A), a kinome screen identifies PIM1 as an inducer of reactivation of latent KSHV. Note that kinase-deficient PIM1-K67M fails to reactivate KSHV.

(B) Sodium butyrate, a chemical inducer of viral reactivation, induces PIM1, which binds to and phosphorylates LANA-1. In the top panel, both sodium butyrate and PIM1 expression induce red fluorescent protein (RFP) expression from viral lytic promoter. In the middle panels, sodium butyrate induces PIM1 expression. In the bottom panels, pull-down western and IP kinase assays indicate that sodium butyrate increases PIM1 association with LANA-1 and phosphorylation of LANA-1 by PIM1.

(C) Several known type I and type II activin and TGFβ receptors (red) are identified in a kinome-wide activin/TGFβ screen. Note that Shh screen hits (green) or BMP receptor kinases (yellow) are not among the strongest effectors.

(D) Similar analysis reveals that the TGFβ screen hits (red) do not affect the Shh pathway reporter.

(E) Analysis of the expression of the identified novel kinases (PIM1, MAP3K10, and DYRK2) in 18 different tissues, compared to 350 other kinases (top). Red indicates high expression and green low or no expression (see Table S6).

found to act downstream of Smo, as it could activate the Shh pathway in Smo-deficient cells (Figure 5A).

Next, we tested whether the kinases act at the level of the GLI transcription factors. Both kinases could modulate the ability of overexpressed Gli2 and GLI1 to induce the Shh pathway (Figures S4B and S4C), and they also could affect activity of GLI in cells lacking the GLI-inhibitory protein SuFu (Figure 5B). These results indicate that both kinases act genetically at the level of GLI. Consistently with the same level of action in the Shh pathway, MAP3K10 and DYRK2 dose-dependently inhibited each others' effect on GLI activity (not shown).

MAP3K10 Modulates the Activity of Gli2 via Regulation of DYRK2 and GSK3β

To further analyze the mechanism by which the kinases act, we tested whether they affect the activity of the transcriptional activator domain of GLI. MAP3K10 failed to further induce transcrip-

tional activity of Gli2 fused to the hyperactive transcriptional activator domain of herpesvirus VP16 (GLI2-VP16) (Figure 5C), indicating that it activates wild-type Gli2 by activating its transcriptional activator domain. In contrast, DYRK2 was able to inactivate also GLI2-VP16 (Figure 5C).

To analyze whether the effect of the kinases on GLI activity was direct, we tested whether coexpression of MAP3K10 or DYRK2 with Gli2 or GLI3 in COS1 cells resulted in phosphorylation of the GLIs. Whereas DYRK2 clearly induced a migration shifts characteristic of phosphorylation, MAP3K10 had no detectable effect on the migration of Gli2 or GLI3 (Figure 5D). To test whether Gli2 is a substrate for DYRK2 or MAP3K10, we used purified kinases in in vitro kinase assays using purified TAP-tagged GLI2 as a substrate. DYRK2 efficiently phosphorylated TAP-GLI2, whereas MAP3K10 failed to do so (Figure 5E).

To identify MAP3K10 binding partners and substrates, biotinylated MAP3K10, and MAP3K10 in the presence of γ^{33}P-ATP
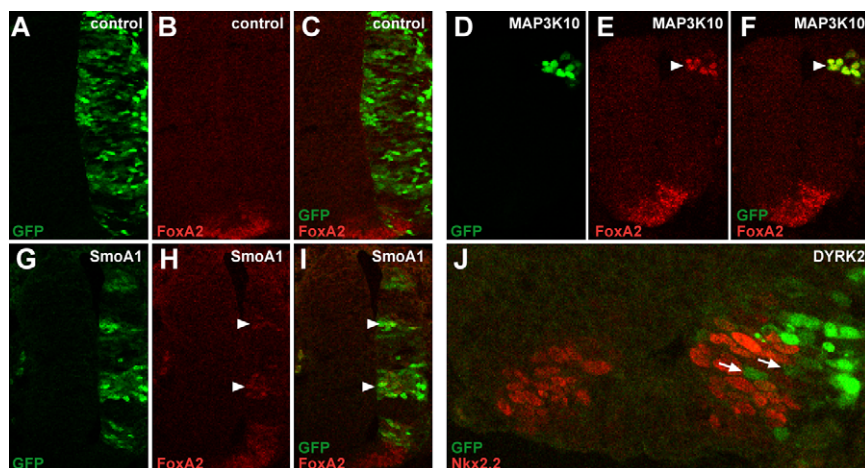
Figure 4. Validation of the Novel Shh Pathway Components

(A–J) MAP3K10 and DYRK2 affect Shh signaling in vivo. Shown are confocal images of antibody-stained sections from neural tubes of chick embryos electroporated with GFP control vector (A–C) or vector coexpressing GFP with activated Smo (SmoA1; G–I), MAP3K10 (D–F), or DYRK2 (J). Note that expression of MAP3K10 or SmoA1 induces ectopic FoxA2 expression (arrowheads), whereas expression of DYRK2 suppresses endogenous Nkx2.2 (arrows). In all panels, ventral side is down. To clearly show individual cells, a merged image of ventral neural tube is shown in (J).

were used to probe-spotted protein microarrays containing 8265 human proteins (Hall et al., 2007). Proteins that bound the highest amount of biotinylated MAP3K10 per mass included DYRK2, and the known Shh pathway regulatory kinases GSK3β, CK1α, and CK1ε (Figure 5F; Table S7). DYRK2 was also phosphorylated by MAP3K10 (Figure 5F); the very high autophosphorylation activity of GSK3β, CK1α, and CK1ε potentially masked phosphorylation by MAP3K10 (Table S7). In kinase assays, purified MAP3K10 increased the activity of GSK3β, but had no effect on activities of CK1α and CK1ε against a casein substrate (Figure 5G).

We further mapped the phosphorylation sites of MAP3K10 on DYRK2 by liquid chromatography-mass spectrometry (LC/MS). Two phosphorylation sites were identified (Figure 5H), including the conserved (Figure S5) threonine 308 in the activation loop. This residue is directly adjacent to tyrosine 309, a critical activating autophosphorylation site found in all DYRK kinases (Figure S6) (Lochhead et al., 2005).

DYRK2 Directly Phosphorylates GLI Proteins and Promotes Their Proteolytic Processing

DYRK2 has been reported to act as a priming kinase to CK1 and GSK-3β (Gwack et al., 2006; Nishi and Lin, 2005) in controlling ubiquitin-mediated degradation of NFAT and OMA-1. CK1 and GSK-3β (Jia et al., 2002; Lum et al., 2003; Price and Kalderon, 2002) have also been linked to the regulation of processing of the *Drosophila* GLI ortholog Ci, suggesting that DYRK2 may act by initiating the phosphorylation events that lead to ubiquitinylation and degradation of Gli2 (Pan et al., 2006), the major transcriptionally activating GLI isoform in NIH 3T3 cells (Varjosalo et al., 2006). DYRK2 and GLI could be coexpressed in COS1 cells, which are not Shh responsive—and which strongly overexpress proteins due to episomal replication of the pCMV6 vector. However, when expressed at more moderate levels in NIH 3T3 cells, cotransfection of DYRK2 resulted in loss of Gli2 (Figure 6A), which could be prevented by the proteasome-inhibitor MG-132 (Figure 6B).

To test whether the kinases affected Gli2 activity by direct phosphorylation, we first mapped the phosphorylation sites of the kinases in Gli2. Purified MAP3K10 failed to phosphorylate fragments of Gli2 expressed in *E.coli*, whereas purified DYRK2

phosphorylated two conserved serines (Ser385 and Ser1011; Figure S7) located in DYRK consensus sequences (Gwack et al., 2006), as indicated by comparison of the results of kinase assays using wild-type fragments and fragments where Ser385 and Ser1011 were mutated to alanine (Figure 6C). Mutation of either of the sites had relatively little effect on the activity of full-length Gli2 (not shown). However, simultaneous mutation of both sites made Gli2 resistant to DYRK2, indicating that DYRK2 affects Gli2 activity via phosphorylation of Ser385 and Ser1011 (Figure 6D). These results indicate that DYRK2 directly phosphorylates Gli2 and induces its degradation by the ubiquitin-proteasome system (Figures 6B and 6D).

DISCUSSION

The Kinome Collection

We report here the molecular cloning of ~93% of all human protein kinases identified in silico by Manning et al. (2002). We further generate a catalytically inactive kinase collection. Together, these collections represent the first high-confidence set of cDNAs representing a large human gene family, and the first systematic collection of functionally altered cDNAs. These collections represent a unique resource for genome-wide studies of signal transduction and signaling crosstalk.

The vast majority (97%; 464/480) of the kinases were cloned directly from human cDNA libraries, resulting in high-quality collection without the mutant, truncated, and/or artifactual clones that can result from the use of PCR or synthetic gene technologies. Analysis of splice variants indicated that the collection does not contain many truncated transcripts, and nearly all (98.1%) known protein domains found in any splice variant of the kinases were present in our collection. This is consistent with our cloning strategy, which generally results in isolation of the most commonly expressed transcript variant. These variants are the most desirable ones for purposes of functional screening. However, due to the complexity of alternative splicing of human genes, it is likely that many functionally important splice variants of kinases will be identified. To facilitate such analyses, splicing of the kinome needs to be analyzed carefully using exon microarrays and/or transcript sequencing of all human tissues.
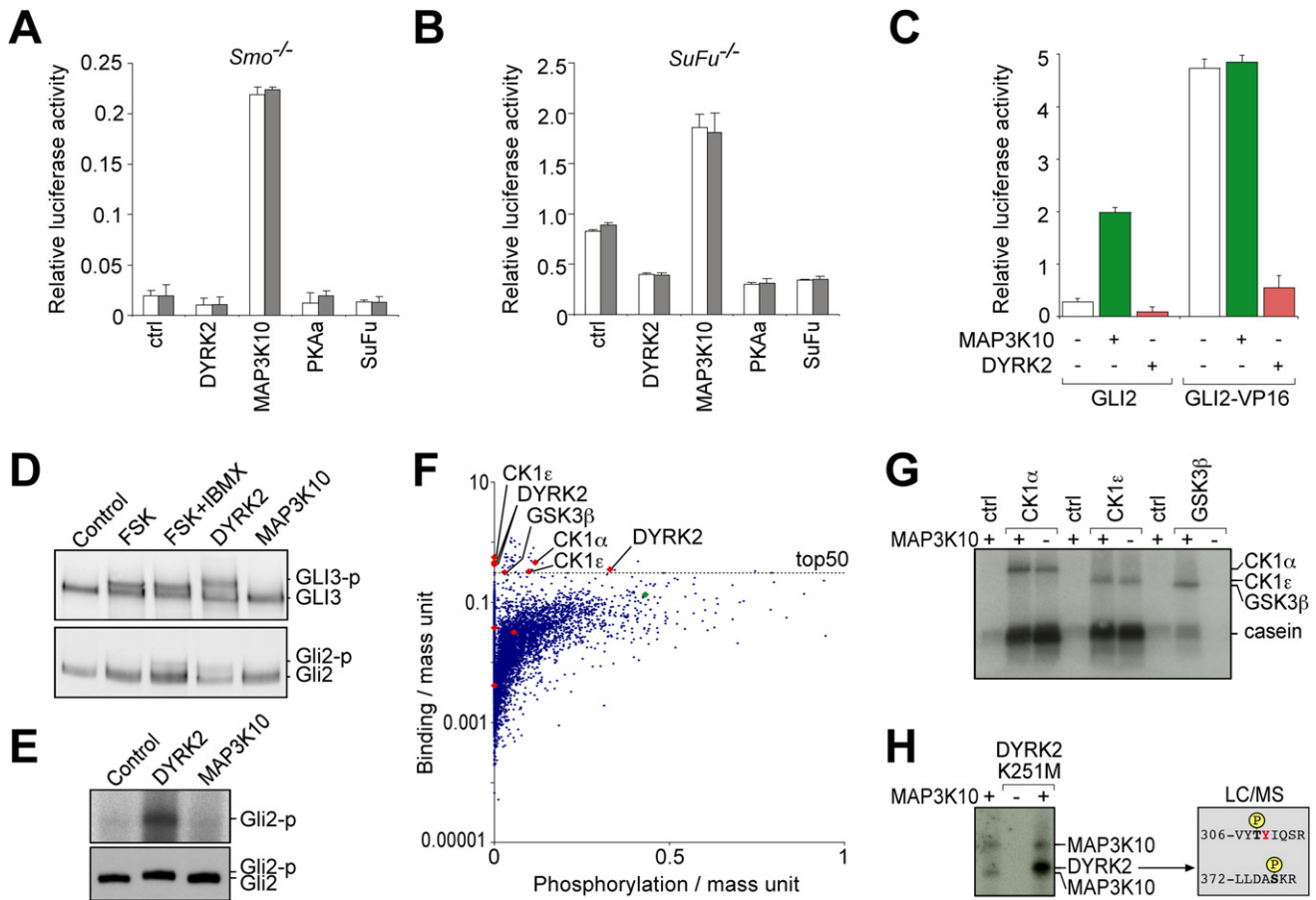
Figure 5. DYRK2 and MAP3K10 Act at the Level of the GLI Transcription Factors

(A and B) Both DYRK2 and MAP3K10 affect activity of the Shh pathway in Smo (A) and SuFu (B) deficient cells indicating that they act downstream of SuFu. PKAa, activated form of PKA. Assays were performed in the absence (white bars) and presence (gray bars) of ShhN. Error bars in all panels indicate 1 SD (n = 4).

(C) GLI2 with hyperactive transcriptional activator domain (GLI2-VP16) is resistant to MAP3K10 but not to DYRK2.

(D) DYRK2 but not MAP3K10 coexpression results in formation of slower migrating forms of GLI2 and GLI3. GLIs phosphorylated by activation of PKA by forskolin (FSK) or FSK and IBMX are shown as control.

(E) DYRK2 but not MAP3K10 phosphorylates full-length Gli2 in vitro. Lower panel shows Gli2 protein loading. Note that the phosphorylation of Gli2 by DYRK2 also results in a slower migrating form as in (D).

(F) Identification of protein-protein interactions and kinase substrates for MAP3K10. In vitro kinase and binding assays were performed using a protein array containing 8265 human proteins. Multiple Hh pathway-related kinases (red diamonds) are among the 50 strongest binding partners (dotted line). Kif3A, a known binding partner for MAP3K10, is also identified as a phosphorylated substrate (green diamond).

(G) MAP3K10 increases the in vitro kinase activity of GSK3β but not CK1α or CK1ε.

(H) DYRK2 is phosphorylated by MAP3K10 to two specific sites as identified by LC/MS. Note that the Thr308 is directly adjacent to the in vivo autophosphorylated tyrosine (red) in DYRK2.

Kinome Expression Screening

To demonstrate the utility of the resource, we used it in three different kinome-wide screens, identifying two novel kinases affecting Shh signaling and one kinase inducing reactivation of a latent human tumor virus, KSHV. These analyses revealed that cDNA expression screening is a powerful and specific method for identification of novel regulators of signaling pathways.

Compared to loss-of-function analyses such as RNAi (Bjorklund et al., 2006; Gwack et al., 2006; Lum et al., 2003), the gain-of-function approach described here can also be used to identify kinases that are not expressed in the cell type tested, act redundantly, or activate the pathways analyzed under path-

ological conditions. In addition, the best models for different cellular signaling events may not be derived from cells of human origin, limiting the utility of human siRNA libraries. Such restriction largely does not limit the use of human cDNA tools in cells from other mammalian species, demonstrated here by the use of the same kinome collection to study kinase signaling in mouse (Shh), mink (TGFβ), and monkey (KSHV) cells.

Identification of Kinases Regulating Mammalian Hh Signaling

Using the kinome library we identified two novel kinases affecting mammalian Shh pathway, MAP3K10 and DYRK2 (Figure 7). The physiological significance of these findings is illustrated by
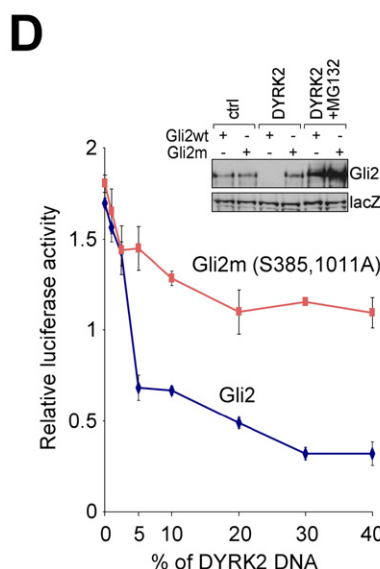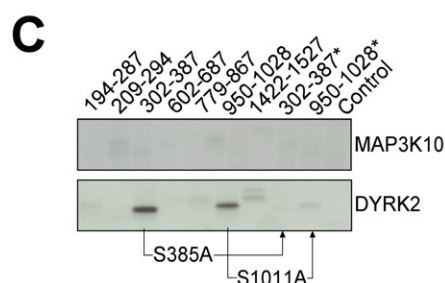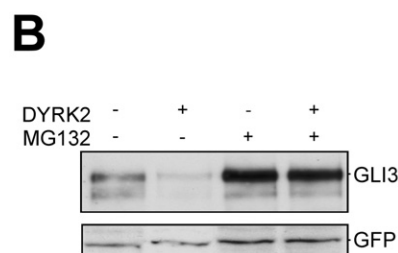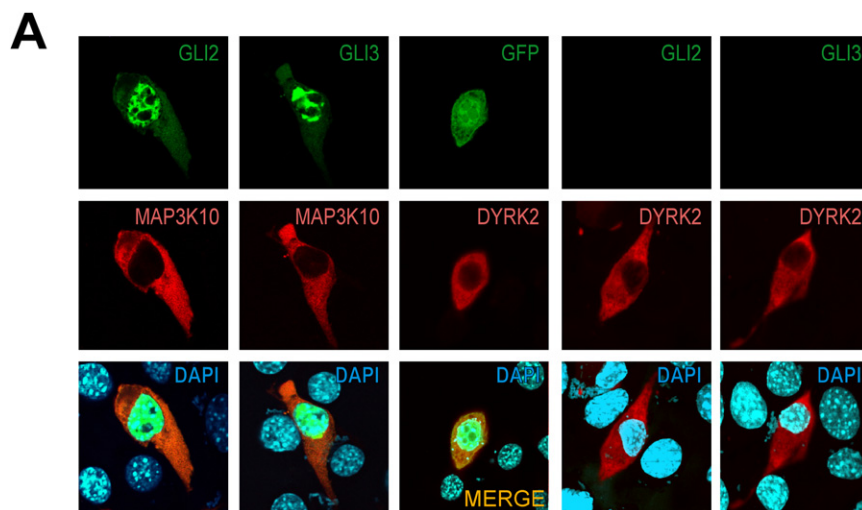
Figure 6. The Mechanisms of Action of DYRK2 and MAP3K10

(A and B) DYRK2 but not MAP3K10 coexpression induces degradation of GLI2 and GLI3 as indicated by immunostaining (A) or western blotting (B) of NIH 3T3 cells 2 days after transfection. Note that MG132 treatment (6 hr) prevents GLI3 degradation (B).

(C) Purified DYRK2 phosphorylates two fragments of GLI2, but fails to phosphorylate the same fragments (arrows) where S385 and S1011 are mutated to alanine. Note that purified MAP3K10 does not phosphorylate any of the GLI2 fragments.

(D) GLI2 lacking the DYRK2 phosphorylation sites (GLI2-S385, 1011A; 5% w/w DNA) is resistant to effects of DYRK2 on its transcriptional activity and protein level (inset). Error bars indicate 1 SD (n = 4).

the facts that both kinases affected Shh signaling also in vivo (Figure 4), and loss of Dyrk2 or Map3k10 function resulted in failure of Shh signaling (Figures 2C, 2D, and S2C). In contrast to other signaling pathways where activation of pathway-specific kinases is central to signal transduction, addition of Shh to responsive cells did not appear to regulate the activity of expressed DYRK2 or MAP3K10. This is consistent with the lack of effect of Hh on activities of CK1α, CK1ε, GSK3β, and PKA, known kinases whose activity is required for Hh signaling in both *Drosophila* and mammals (Varjosalo and Taipale, 2007). The mechanism by which the Shh signal is transduced thus appears to depend on multiple relatively generic kinases, with activity of the pathway likely controlled by access of these kinases to pathway-specific substrate(s) (Figure 7).

In contrast to the nuclear kinase DYRK1, which has been reported to activate GLI (Mao et al., 2002), we found that DYRK2 localizes to the cytoplasm and inhibits Shh signaling by decreasing GLI activity. DYRK2 directly phosphorylated Gli2 sequences and resulted in the loss of coexpressed GLI proteins, indicating

that DYRK2 acts by inducing the phosphorylation and degradation of GLI proteins via the ubiquitin/proteasome pathway (Figure 6).

The other kinase we identified, MAP3K10, acts positively on the Shh pathway by increasing the transcriptional activator activity of GLI (Figure 5C). MAP3K10 has previously been linked to JNK (C-Jun N-terminal kinase) signaling (Gallo and Johnson, 2002) and to regulation of trafficking of clathrin-coated vesicles (Akbarzadeh et al., 2002). The effect of MAP3K10 on GLI2 appears not to be direct. Instead, MAP3K10 binds to multiple kinases regulating Shh pathway, including CK1α, CK1ε, GSK3β, and DYRK2. In addition, MAP3K10 has been shown to associate with Kif3a (Nagata et al., 1998), a component of cytoplasmic kinesin II, which is required for Shh pathway regulation in mice (Huangfu et al., 2003). Our protein microarray experiments confirmed this finding and further indicated that Kif3a is also a substrate for MAP3K10. Although both MAP3K10 and DYRK2 act at the level of Gli2 but with opposing effects, MAP3K10 action cannot be explained solely by its effect on DYRK2, as these kinases have different activity on Gli2-VP16 transcriptional activity (Figure 5C). Many connections of MAP3K10 with different pathway components suggest that MAP3K10 action on GLI2 is likely to be complex, and its detailed dissection will require further mechanistic studies.

Viral Reactivation Screen

Our kinome-wide ectopic expression screen identified PIM1 as a novel kinase regulating the balance between latency and lytic replication in KSHV-infected cells. PIM kinases have previously been linked to regulation of viral oncogenesis. PIM1 and PIM2 have been suggested to promote EBV-induced immortalization
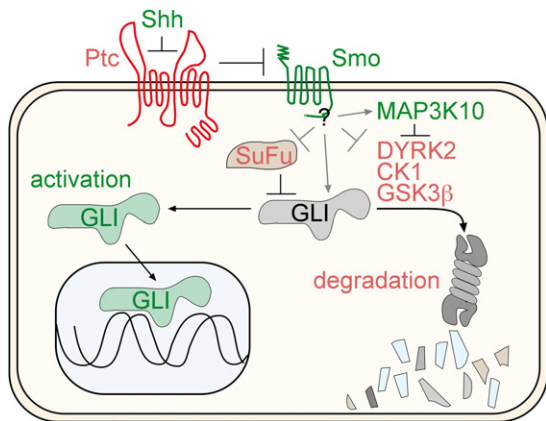
Figure 7. A Model of MAP3K10 and DYRK2 Function
Green and red colors indicate positively and negatively acting components of the Shh pathway, respectively.

and tumorigenesis (Rainio et al., 2005), and PIM1 was proposed to be involved in KSHV pathogenesis via its interaction and phosphorylation of KSHV latency-associated nuclear antigen (LANA-1) (Bajaj et al., 2006). We show here that viral reactivation induces PIM1 expression and activity, resulting in LANA-1 binding to and phosphorylation by PIM1, and consequent conversion of KSHV from latency to lytic replication.

The switch from latency to lytic replication is an elementary decision in viral life cycle—especially in the case of herpes viruses. Several lines of evidence support the importance of induction of viral replication in herpes viral tumorigenesis (Grundhoff and Ganem, 2004; Hayward et al., 2006). Hence, cellular signaling pathways operative during viral reactivation could represent potential novel targets for therapeutic intervention.

TGFβ Screen

In TGFβ screen we identified type I and type II receptors for activin and TGFβ, but did not find any novel kinases. This is consistent with the fact that the TGFβ pathway is relatively well characterized and short – TGFβ type I receptors directly phosphorylate the Smad transcription factors (Massague et al., 2005). However, the clear identification of the TGFβ receptors in this screen establishes that overexpression screening is a highly sensitive and accurate method in identifying critical pathway components.

Signaling Crosstalk

Previous biochemical and genetic studies have revealed that in addition to functioning on their specific pathways, many kinases can also participate in crosstalk between signaling pathways (e.g., Cully et al., 2006; Katz et al., 2007). However, signaling crosstalk induced by overexpression has generally not been systematically analyzed. Our kinome screens, in fact, represent the first genome-wide quantitative analyses of crosstalk between kinase pathways. A large number of overexpressed kinases, which normally function in their specific pathways, had statistically significant effects in both the Shh and TGFβ screens. These results indicate that there can be extensive crosstalk between different signaling pathways under pathological conditions where kinases

are overexpressed and/or strongly activated. In an analogous manner, activation of signaling pathways controlling cell growth by mutant kinases, which normally do not act on such pathways, could explain the recent observations that an unexpectedly large number of protein kinases are found to be mutated in human cancer (Greenman et al., 2007).

The extensive crosstalk observed also explains the large number of published results where gain-of-function experiments have suggested a role for specific proteins in different pathways, but the corresponding loss-of-function experiments have failed to corroborate the findings (e.g., Lange-Carter et al., 1993; Lee et al., 1997; Merchant et al., 2005; Murone et al., 2000; Yan et al., 1994; Yujiri et al., 2000). However, we find here that the known kinases affecting a given pathway generally have a very strong effect compared to the other kinases (see also Lange-Carter et al., 1993; Yan et al., 1994; Yujiri et al., 2000), and thus by analyzing a large set of gain-of-function experiments at the same time, one can focus on the strongest effectors whose effects are more likely to be significant under physiological conditions.

EXPERIMENTAL PROCEDURES

Generation of Kinome-wide Expression-Ready cDNA Libraries
The full-length kinase cDNA clones were identified using sequencing of 800,000 random clones, followed by isolation of specific clones using Rapid-Screen Arrayed cDNA Panels (He and Jay, 2001), and finally by PCR (see Supplemental Experimental Procedures). To generate Gateway clones, the ORFs were recombined to pDONR221 and sequence verified. The active site residues (Table S2) were mutated using "quick-change" site-directed mutagenesis (Stratagene).

Cell Culture and Transfection
Cells were cultured in DMEM containing 10% fetal bovine serum (Mv1Lu, 293-ShhN, COS1, s4$^{Smo-/-}$ [Varjosalo et al., 2006] and SuFu$^{-/-}$ [Svard et al., 2006] mouse embryonic fibroblasts) or 10% bovine calf serum (NIH 3T3 and Shh-LIGHT2) and antibiotics. SuFu$^{-/-}$ MEFs (SuFuMEF/E174-2/5) were from R. Toftgård. Transfection was performed according to manufacturers' instructions; FuGene6 was used for NIH 3T3, Vero, SuFu$^{-/-}$ and s4$^{Smo-/-}$ cells, Hi-Perfect for Shh-LIGHT2, and JetPEI for COS1 cells. Chicken embryos were electroporated (Intracel TSS20 Ovodyne; 30 V pulses for 5 × 50 ms at 4 mm electrode distance) at Hamburger-Hamilton stage 11 and fixed by PFA after 42–48 hr (stage 18 and 19).

Screening and Data Analysis
All screens were performed on 96-well plate format. Luciferase-reporter screening was performed in NIH 3T3 cells (Shh) or Mv1Lu cells (activin/TGFβ) essentially as described (Dennler et al., 1998; Taipale et al., 2002), using 50 ng of kinase constructs and 50 ng of reporters (1:19 mix of control to pathway reporter) per well. pRL-SV40 (Promega) was used as a control reporter, and Gli-Luc (Taipale et al., 2002) and pCAGA-Luc (Dennler et al., 1998) were used as specific reporters for Shh and activin/TGFβ pathway, respectively. After 1 day (activin/TGFβ) or 2 days (Shh) transfection using FuGENE 6, cells were stimulated with TGFβ3 (5 ng/ml; a kind gift from Dr. Peter ten Dijke) or ShhN (from 293-ShhN cell-conditioned medium [Chen et al., 2002], 1:10 v/v) in medium containing 0.5% serum. After 16 hr (activin/TGFβ) or 2 days (Shh), firefly and *Renilla* luciferase activities were determined using the dual-Luciferase kit (Promega; BMG FLUOstar OPTIMA Luminometer), followed by subtraction of background luminescence counts from untransfected cells. Relative luciferase activities were calculated by dividing the pathway-specific firefly luciferase counts by the control *Renilla* luciferase counts separately for all replicates, and sample mean and SD were calculated from these values (n = 3). Constructs that caused a severe drop in *Renilla* luciferase counts (Tables S3 and S5) were classified as toxic and were not analyzed further. The high and

low value ranges (±3 SD) that should contain less than one kinase sample if no kinases were active was determined by including multiple control samples expressing GFP (pEGFP-C1).

Four siRNAs from QIAGEN mouse kinome siRNA set v 1.0 targeting the same kinases were pooled and transfected to Shh-LIGHT2 reporter cells. After 2 days, the cells were treated or not with conditioned medium containing Shh, and luciferase activities measured after 60 hr.

For the viral-reactivation screen, Vero cells infected with rKSHV.219 virus were transfected with individual kinase cDNAs. After 48 hr, the cells were treated with recombinant baculovirus (BacK50) expressing the KSHV lytic activator ORF 50 (RTA; a gift from J. Vieira) for 2 hr. For positive control of maximal reactivation, the cells were treated with 1.25 mM sodium butyrate (Sigma). After 30 hr, the cells were fixed with PFA and RFP intensity was analyzed by Cellomics Arrayscan 4.5 microscope.

For analysis of kinase expression, data from HG-U133a Affymetrix human gene-expression microarray analyses were collected from GeneExpression Omnibus, ArrayExpress, and scientific journals, and the data integrated and normalized to ensure comparability (S.K. and O.K., unpublished data).

Immunochemistry, Fluorescence Microscopy, and Kinase Assays

Antibodies used are described in Supplemental Experimental Procedures. For immunoblotting, samples were transferred to nitrocellulose, blocked, incubated with anti-V5 (tagged kinases) or anti-Myc-epitope (Myc-GLI3 fusion protein) antibodies, followed by HRP-conjugated secondary antibodies and chemiluminescent detection (Amersham ECL).

For immunochemistry, PFA-fixed cells in microwell plates (Perkin Elmer Viewplate) and 10 μm cryosections were incubated with the indicated antibodies followed by Alexa594-conjugated secondary antibodies. Fluorescent fusion proteins expressed in NIH 3T3 cells grown on fibronectin-coated coverslips (BD Biosciences) were observed 2 days after transfection. Imaging was performed using Cellomics Arrayscan, Zeiss AxioplanII, or Zeiss LSM510 Meta confocal microscopes.

ProtoArray v 4.0 arrays were used for protein array-based interaction and kinase assays (Invitrogen). In-solution kinase assays were performed using purified E. coli expressed DYRK2-MBP or insect cell expressed MAP3K10-GST, CK1α-GST, CK1ε-His6, and GSK3β-His6 (Invitrogen) fusion proteins and purified casein, TAP-Gli2 or GST-Gli2 fragment substrates (see Supplemental Experimental Procedures). Samples were incubated for 1 hr at 30°C, separated by SDS-PAGE, transferred to nitrocellulose, and exposed to Hypermax MR film (Kodak). For LC/MS analyses, substrates were separated by SDS-PAGE, and trypsin digested, followed by enrichment of phosphorylated peptides by TiO2 beads (Thingholm et al., 2006) and analysis by nanoLC FT-MS (Thermo Electron).

SUPPLEMENTAL DATA

Supplemental Data include seven figures, seven tables, Supplemental Experimental Procedures, Supplemental References, and a Supplemental Database and can be found with this article online at http://www.cell.com/cgi/content/full/133/3/537/DC1/.

REFERENCES

Akbarzadeh, S., Ji, H., Frecklington, D., Marmy-Conus, N., Mok, Y.F., Bowes, L., Devereux, L., Linsenmeyer, M., Simpson, R.J., and Dorow, D.S. (2002). Mixed lineage kinase 2 interacts with clathrin and influences clathrin-coated vesicle trafficking. J. Biol. Chem. 277, 36280–36287.

Bajaj, B.G., Verma, S.C., Lan, K., Cotter, M.A., Woodman, Z.L., and Robertson, E.S. (2006). KSHV encoded LANA upregulates Pim-1 and is a substrate for its kinase activity. Virology 351, 18–28.

Bjorklund, M., Taipale, M., Varjosalo, M., Saharinen, J., Lahdenpera, J., and Taipale, J. (2006). Identification of pathways regulating cell size and cell-cycle progression by RNAi. Nature 439, 1009–1013.

Cesarman, E., Chang, Y., Moore, P.S., Said, J.W., and Knowles, D.M. (1995). Kaposi's sarcoma-associated herpesvirus-like DNA sequences in AIDS-related body-cavity-based lymphomas. N. Engl. J. Med. 332, 1186–1191.

Chang, Y., Cesarman, E., Pessin, M.S., Lee, F., Culpepper, J., Knowles, D.M., and Moore, P.S. (1994). Identification of herpesvirus-like DNA sequences in AIDS-associated Kaposi's sarcoma. Science 266, 1865–1869.

Chen, J.K., Taipale, J., Young, K.E., Maiti, T., and Beachy, P.A. (2002). Small molecule modulation of Smoothened activity. Proc. Natl. Acad. Sci. USA 99, 14071–14076.

Chen, M.H., Gao, N., Kawakami, T., and Chuang, P.T. (2005). Mice deficient in the fused homolog do not exhibit phenotypes indicative of perturbed hedgehog signaling during embryonic development. Mol. Cell. Biol. 25, 7042–7053.

Cooper, A.F., Yu, K.P., Brueckner, M., Brailey, L.L., Johnson, L., McGrath, J.M., and Bale, A.E. (2005). Cardiac and CNS defects in a mouse with targeted disruption of suppressor of fused. Development 132, 4407–4417.

Cully, M., You, H., Levine, A.J., and Mak, T.W. (2006). Beyond PTEN mutations: the PI3K pathway as an integrator of multiple inputs during tumorigenesis. Nat. Rev. Cancer 6, 184–192.

Dennler, S., Itoh, S., Vivien, D., ten Dijke, P., Huet, S., and Gauthier, J.M. (1998). Direct binding of Smad3 and Smad4 to critical TGF beta-inducible elements in the promoter of human plasminogen activator inhibitor-type 1 gene. EMBO J. 17, 3091–3100.

Futreal, P.A., Coin, L., Marshall, M., Down, T., Hubbard, T., Wooster, R., Rahman, N., and Stratton, M.R. (2004). A census of human cancer genes. Nat. Rev. Cancer 4, 177–183.

Gallo, K.A., and Johnson, G.L. (2002). Mixed-lineage kinase control of JNK and p38 MAPK pathways. Nat. Rev. Mol. Cell Biol. 3, 663–672.

Greenman, C., Stephens, P., Smith, R., Dalgliesh, G.L., Hunter, C., Bignell, G., Davies, H., Teague, J., Butler, A., Stevens, C., et al. (2007). Patterns of somatic mutation in human cancer genomes. Nature 446, 153–158.

Grundhoff, A., and Ganem, D. (2004). Inefficient establishment of KSHV latency suggests an additional role for continued lytic replication in Kaposi sarcoma pathogenesis. J. Clin. Invest. 113, 124–136.

Gwack, Y., Sharma, S., Nardone, J., Tanasa, B., Iuga, A., Srikanth, S., Okamura, H., Bolton, D., Feske, S., Hogan, P.G., and Rao, A. (2006). A genome-wide Drosophila RNAi screen identifies DYRK-family kinases as regulators of NFAT. Nature 441, 646–650.

Hall, D.A., Ptacek, J., and Snyder, M. (2007). Protein microarray technology. Mech. Ageing Dev. 128, 161–167.

Hayward, S.D., Liu, J., and Fujimuro, M. (2006). Notch and Wnt signaling: mimicry and manipulation by gamma herpesviruses. Sci. STKE 2006, re4.

He, W.-W., and Jay, G. (2001). Rapid-screen cDNA library panels. U.S. patent 6316193. November 2001.

Huangfu, D., Liu, A., Rakeman, A.S., Murcia, N.S., Niswander, L., and Anderson, K.V. (2003). Hedgehog signalling in the mouse requires intraflagellar transport proteins. Nature 426, 83–87.

Huse, M., and Kuriyan, J. (2002). The conformational plasticity of protein kinases. Cell 109, 275–282.

Jacob, J., and Briscoe, J. (2003). Gli proteins and the control of spinal-cord patterning. EMBO Rep. 4, 761–765.

Jia, J., Amanai, K., Wang, G., Tang, J., Wang, B., and Jiang, J. (2002). Shaggy/GSK3 antagonizes Hedgehog signalling by regulating Cubitus interruptus. Nature 416, 548–552.

Kalderon, D. (2005). The mechanism of hedgehog signal transduction. Biochem. Soc. Trans. 33, 1509–1512.

Katz, M., Amit, I., and Yarden, Y. (2007). Regulation of MAPKs by growth factors and receptor tyrosine kinases. Biochim. Biophys. Acta 1773, 1161–1176.

Lange-Carter, C.A., Pleiman, C.M., Gardner, A.M., Blumer, K.J., and Johnson, G.L. (1993). A divergence in the MAP kinase regulatory network defined by MEK kinase and Raf. Science 260, 315–319.

Lee, F.S., Hagler, J., Chen, Z.J., and Maniatis, T. (1997). Activation of the IkappaB alpha kinase complex by MEKK1, a kinase of the JNK pathway. Cell 88, 213–222.

Lochhead, P.A., Sibbet, G., Morrice, N., and Cleghon, V. (2005). Activation-loop autophosphorylation is mediated by a novel transitional intermediate form of DYRKs. Cell 121, 925–936.

Lum, L., Yao, S., Mozer, B., Rovescalli, A., Von Kessler, D., Nirenberg, M., and Beachy, P.A. (2003). Identification of Hedgehog pathway components by RNAi in Drosophila cultured cells. Science 299, 2039–2045.

Manning, G., Whyte, D.B., Martinez, R., Hunter, T., and Sudarsanam, S. (2002). The protein kinase complement of the human genome. Science 298, 1912–1934.

Mao, J., Maye, P., Kogerman, P., Tejedor, F.J., Toftgard, R., Xie, W., Wu, G., and Wu, D. (2002). Regulation of Gli1 transcriptional activity in the nucleus by Dyrk1. J. Biol. Chem. 277, 35156–35161.

Massague, J., Seoane, J., and Wotton, D. (2005). Smad transcription factors. Genes Dev. 19, 2783–2810.

Mendenhall, M.D., Richardson, H.E., and Reed, S.I. (1988). Dominant negative protein kinase mutations that confer a G1 arrest phenotype. Proc. Natl. Acad. Sci. USA 85, 4426–4430.

Merchant, M., Evangelista, M., Luoh, S.M., Frantz, G.D., Chalasani, S., Carano, R.A., van Hoy, M., Ramirez, J., Ogasawara, A.K., McFarland, L.M., et al. (2005). Loss of the serine/threonine kinase fused results in postnatal growth defects and lethality due to progressive hydrocephalus. Mol. Cell. Biol. 25, 7054–7068.

Murone, M., Luoh, S.M., Stone, D., Li, W., Gurney, A., Armanini, M., Grey, C., Rosenthal, A., and de Sauvage, F.J. (2000). Gli regulation by the opposing activities of fused and suppressor of fused. Nat. Cell Biol. 2, 310–312.

Nagata, K., Puls, A., Futter, C., Aspenstrom, P., Schaefer, E., Nakata, T., Hirokawa, N., and Hall, A. (1998). The MAP kinase kinase kinase MLK2 co-localizes with activated JNK along microtubules and associates with kinesin superfamily motor KIF3. EMBO J. 17, 149–158.

Nishi, Y., and Lin, R. (2005). DYRK2 and GSK-3 phosphorylate and promote the timely degradation of OMA-1, a key regulator of the oocyte-to-embryo transition in C. elegans. Dev. Biol. 288, 139–149.

Nolen, B., Taylor, S., and Ghosh, G. (2004). Regulation of protein kinases; controlling activity through activation segment conformation. Mol. Cell 15, 661–675.

Pan, Y., Bai, C.B., Joyner, A.L., and Wang, B. (2006). Sonic hedgehog signaling regulates Gli2 transcriptional activity by suppressing its processing and degradation. Mol. Cell. Biol. 26, 3365–3377.

Price, M.A., and Kalderon, D. (2002). Proteolysis of the Hedgehog signaling effector Cubitus interruptus requires phosphorylation by Glycogen Synthase Kinase 3 and Casein Kinase 1. Cell 108, 823–835.

Rainio, E.M., Ahlfors, H., Carter, K.L., Ruuska, M., Matikainen, S., Kieff, E., and Koskinen, P.J. (2005). Pim kinases are upregulated during Epstein-Barr virus infection and enhance EBNA2 activity. Virology 333, 201–206.

Riobo, N.A., Haines, G.M., and Emerson, C.P., Jr. (2006a). Protein kinase C-delta and mitogen-activated protein/extracellular signal-regulated kinase-1 control GLI activation in hedgehog signaling. Cancer Res. 66, 839–845.

Riobo, N.A., Lu, K., Ai, X., Haines, G.M., and Emerson, C.P., Jr. (2006b). Phosphoinositide 3-kinase and Akt are essential for Sonic Hedgehog signaling. Proc. Natl. Acad. Sci. USA 103, 4505–4510.

Rubin, L.L., and de Sauvage, F.J. (2006). Targeting the Hedgehog pathway in cancer. Nat. Rev. Drug Discov. 5, 1026–1033.

Svard, J., Heby-Henricson, K., Persson-Lek, M., Rozell, B., Lauth, M., Bergstrom, A., Ericson, J., Toftgard, R., and Teglund, S. (2006). Genetic elimination of Suppressor of fused reveals an essential repressor function in the mammalian Hedgehog signaling pathway. Dev. Cell 10, 187–197.

Taipale, J., Chen, J.K., Cooper, M.K., Wang, B., Mann, R.K., Milenkovic, L., Scott, M.P., and Beachy, P.A. (2000). Effects of oncogenic mutations in Smoothened and Patched can be reversed by cyclopamine. Nature 406, 1005–1009.

Taipale, J., Cooper, M.K., Maiti, T., and Beachy, P.A. (2002). Patched acts catalytically to suppress the activity of Smoothened. Nature 418, 892–897.

Thingholm, T.E., Jorgensen, T.J., Jensen, O.N., and Larsen, M.R. (2006). Highly selective enrichment of phosphorylated peptides using titanium dioxide. Nat. Protocols 1, 1929–1935.

Varjosalo, M., and Taipale, J. (2007). Hedgehog signaling. J. Cell Sci. 120, 3–6.

Varjosalo, M., Li, S.P., and Taipale, J. (2006). Divergence of hedgehog signal transduction mechanism between Drosophila and mammals. Dev. Cell 10, 177–186.

Venter, J.C., Adams, M.D., Myers, E.W., Li, P.W., Mural, R.J., Sutton, G.G., Smith, H.O., Yandell, M., Evans, C.A., Holt, R.A., et al. (2001). The sequence of the human genome. Science 291, 1304–1351.

Vieira, J., and O'Hearn, P.M. (2004). Use of the red fluorescent protein as a marker of Kaposi's sarcoma-associated herpesvirus lytic gene expression. Virology 325, 225–240.

Yan, M., Dai, T., Deak, J.C., Kyriakis, J.M., Zon, L.I., Woodgett, J.R., and Templeton, D.J. (1994). Activation of stress-activated protein kinase by MEKK1 phosphorylation of its activator SEK1. Nature 372, 798–800.

Yujiri, T., Ware, M., Widmann, C., Oyer, R., Russell, D., Chan, E., Zaitsu, Y., Clarke, P., Tyler, K., Oka, Y., et al. (2000). MEK kinase 1 gene disruption alters cell migration and c-Jun NH2-terminal kinase regulation but does not cause a measurable defect in NF-kappa B activation. Proc. Natl. Acad. Sci. USA 97, 7272–7277.

Zhou, Q., Apionishev, S., and Kalderon, D. (2006). The contributions of Protein Kinase A and Smoothened phosphorylation to Hedgehog signal transduction in Drosophila melanogaster. Genetics 173, 2049–2062.